

# Boron-Doped Carbon Nanotubes as Metal-Free Electrocatalysts for the Oxygen Reduction Reaction\*\*

Lijun Yang, Shujuan Jiang, Yu Zhao, Lei Zhu, Sheng Chen, Xizhang Wang, Qiang Wu, Jing Ma, Yanwen Ma,\* and Zheng Hu\*

Fuel cells are clean, sustainable energy conversion devices for power generation, and they most commonly use platinum as the electrocatalyst.<sup>[1]</sup> However, Pt-based catalysts suffer from very limited reserves, high cost, and inactivation by CO poisoning; these are major obstacles that fuel cells have to overcome for commercialization.<sup>[1–6]</sup> Thus, exploring non-precious metal or even metal-free catalysts to rival platinum in activity and durability is absolutely crucial, with a potentially revolutionary impact on fuel-cell technologies. Very recently, metal-free PEDOT<sup>[6]</sup> and nitrogen-doped carbon nanotubes (NCNTs)<sup>[7,8]</sup> have shown a striking electrocatalytic performance for the oxygen reduction reaction (ORR). These breakthroughs have activated an exciting field for exploring the advanced metal-free electrocatalysts and understanding the related mechanism.

As one of the most important carbon nanostructures, carbon-based nanotubes have been widely studied as the support of electrocatalysts for fuel cells in recent years.<sup>[9–12]</sup> Recent progress involving doping carbon nanotubes (CNTs) with electron-rich nitrogen to transform CNTs into superb metal-free electrocatalysts for the ORR<sup>[7,8]</sup> has motivated our curiosity to examine the corresponding performance of its counterpart by doping CNTs with electron-deficient boron. Intuitively, the adsorption of O<sub>2</sub> on boron dopant should be quite easy owing to the large difference of electronegativity between boron and oxygen, which is the precondition for the subsequent O<sub>2</sub> dissociation. In this study, BCNTs with tunable boron content of 0–2.24 atom % were synthesized. The ORR

onset and peak potentials shift positively and the current density increases noticeably with increasing boron content, indicating a strong dependence of the ORR performance on boron content. Moreover, the origin of the electrocatalytic activity of BCNTs including the role of the boron dopant has been revealed by density functional theory (DFT) calculations. The experimental and theoretical results provide a new strategy to explore carbon-based metal-free electrocatalysts that are significant to the development of fuel cells.

Using chemical vapor deposition (CVD) with benzene, triphenylborane (TPB), and ferrocene as precursors and catalyst, BCNTs were synthesized with tunable boron content of 0–2.24 at % by using different TPB concentrations. BCNTs with boron content of 0.86, 1.33, and 2.24 at %, as determined by X-ray photoelectron spectroscopy (XPS), were denoted as B<sub>1</sub>CNTs, B<sub>2</sub>CNTs, and B<sub>3</sub>CNTs, respectively (Supporting Information, S1.1). Boron doping into CNTs will lead to the broken hexagonal symmetry of graphite, and thus induce an increased D band in the Raman spectrum<sup>[13–17]</sup> (Figure 1). The

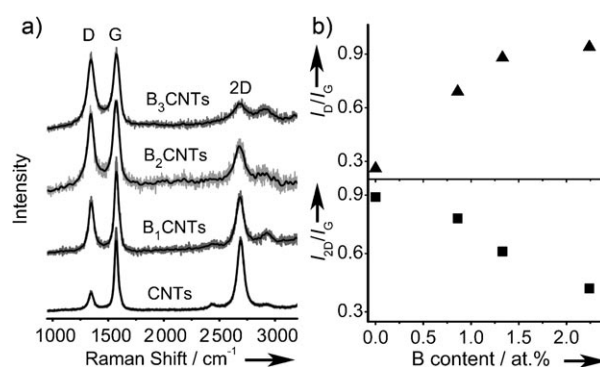


**Figure 1.** Raman spectra and derived parameters. a) Raman spectra for CNTs, B<sub>1</sub>CNTs, B<sub>2</sub>CNTs, and B<sub>3</sub>CNTs. Lines are fitted to the data. b) The derived profiles of  $I_D/I_G$  (▲) and  $I_{2D}/I_G$  (■) versus boron content.

ratio of the D mode and G mode intensities ( $I_D/I_G$ ) increases, while that of the 2D and G mode ( $I_{2D}/I_G$ ) decreases with increasing boron dopant (Figure 1b), accompanied by the gradual red-shift of the 2D peaks<sup>[15–17]</sup> (Figure 1a). These results indicate that the boron-doped CNTs with tunable boron content have been successfully prepared, which provides us a suitable platform for exploring the electrocatalytic performance of BCNTs for the ORR (Supporting Information, S2).

The electrocatalytic capabilities of these samples were first evaluated by cyclic voltammetry (CV; Figure 2a). With

[\*] Dr. L. Yang,<sup>[†]</sup> Dr. S. Jiang,<sup>[†]</sup> Y. Zhao,<sup>[†]</sup> L. Zhu, S. Chen, Prof. X. Wang, Prof. Q. Wu, Prof. J. Ma, Prof. Y. Ma, Prof. Z. Hu  
Key Laboratory of Mesoscopic Chemistry of MOE and  
Jiangsu Provincial Lab for Nanotechnology  
Institute of Theoretical and Computational Chemistry  
School of Chemistry and Chemical Engineering  
Nanjing University, Nanjing, 210093 (China)  
E-mail: zhenghu@nju.edu.cn

Prof. Y. Ma

Jiangsu Key Lab for Organic Electronics and Information Displays  
Institute of Advanced Materials

Nanjing University of Posts and Telecommunications  
Nanjing, 210046 (China)

E-mail: iamywma@njupt.edu.cn

[†] These authors contributed equally to this work.

[\*\*] This work was jointly supported by the NSFC (20833002, 21073085), the “973” program (2007CB936300), the program for Changjiang Scholars and Innovative Research Team in University (PCSIRT), and the Jiangsu Postdoctoral Foundation (1001004C). We thank Prof. Songqing Liu for the helpful discussion on electrochemical analysis.

Supporting information for this article is available on the WWW under <http://dx.doi.org/10.1002/anie.201101287>.

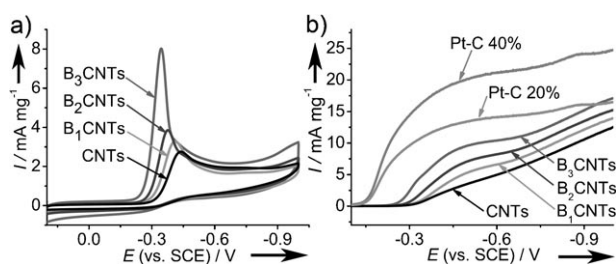


**Figure 2.** Electrocatalytic capabilities of the BCNT catalysts for the ORR in  $O_2$ -saturated 1 M NaOH electrolyte. a) CV curves (scan rate  $50 \text{ mVs}^{-1}$ ). b) RDE voltammetry with a rotation speed of 2500 rpm (scan rate  $10 \text{ mVs}^{-1}$ ). For comparison, corresponding examinations for CNTs and commercial Pt/C catalysts (20 and 40 wt% Pt loading) were also carried out.

increasing boron content, the maximum peak current clearly increases from 2.8 (CNTs) to 3.2 ( $B_1$ CNTs), 3.8 ( $B_2$ CNTs), and  $8.0 \text{ mA mg}^{-1}$  ( $B_3$ CNTs), accompanied by a progressive positive shift of the peak potentials from  $-0.43$  (CNTs) to  $-0.41$  ( $B_1$ CNTs),  $-0.38$  ( $B_2$ CNTs), and  $-0.35 \text{ V}$  ( $B_3$ CNTs) in reference to the saturated calomel electrode (SCE). Similar evolutions are also observed for the steady-state diffusion currents and the on-set and half-wave potentials in rotating disk electrode (RDE) voltammetry (Figure 2b). These results indicate that the electrocatalytic activities of the catalysts for the ORR increase with increasing boron content, with the highest activity for  $B_3$ CNT catalyst. Furthermore, rotating ring-disk electrode (RRDE) measurements reveal that the transferred electron number per oxygen molecule involved in ORR increases slightly from 2.2 for CNTs to 2.5 for  $B_3$ CNTs, indicating a dominant two-electron process (Supporting Information, S3). From these experimental data, it is concluded that the much improved catalytic performance of BCNTs with respect to CNTs originates from the boron doping (Supporting Information, S4). Though the present performance of BCNTs is not yet as good as the commercial Pt/C catalyst (Figure 2b), the proportional relationship between ORR performance and boron content suggests the great potential of BCNTs for further improvement.

Along with the electrocatalytic activity for the ORR, the  $B_3$ CNT catalyst presents excellent stability and immunity towards methanol crossover and CO poisoning, which overcomes another main challenge faced by the metal-based catalysts in fuel cells. The chronoamperometric responses to methanol or CO introduced into the  $O_2$ -saturated electrolyte were performed for  $B_3$ CNT and Pt/C catalysts (Figure 3). After the addition of 1.5 mL of methanol, the ORR current for  $B_3$ CNT catalyst does not show obvious change; in contrast, the ORR current for the Pt/C catalyst suffers a sharp decrease and even changes to a negative current as a result of the mixed potential<sup>[18,19]</sup> (Figure 3a). When additional CO with the same flow of  $O_2$  is introduced, the ORR current for Pt/C is greatly weakened by about 56.9% from 130 to  $56 \mu\text{A}$ , which is much larger than the decrease by about 26.3% for  $B_3$ CNTs (Figure 3b). The great current decrease for Pt/C mainly results from the CO poisoning, while the small decrease for  $B_3$ CNTs is from the decreased solubility of  $O_2$  in the electrolyte owing to the decreased partial pressure

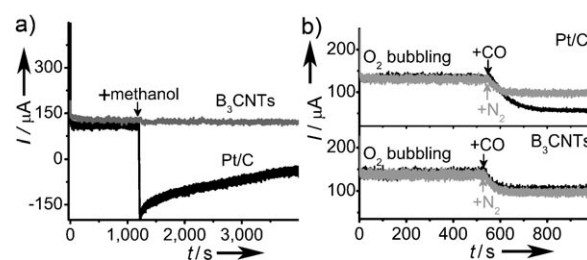


**Figure 3.** Chronoamperometric responses in the  $O_2$ -saturated electrolyte for Pt/C (black) and  $B_3$ CNT (dark gray) catalysts. a) Methanol crossover tests by introducing 1.5 mL methanol into the electrolyte at 1200 s. b) CO poisoning tests by introducing additional CO with the same flow of  $O_2$  into the electrolyte at 520 s. Parallel experiments for Pt/C (40 wt% Pt loading) and  $B_3$ CNT catalysts are carried out by replacing CO with the same flow of  $N_2$  (light gray).

of  $O_2$  (Henry's Law).<sup>[20,21]</sup> This result is confirmed by the results of replacing the CO with the same flow of  $N_2$  to eliminate the poisoning effect. On introducing  $N_2$ , the ORR current for Pt/C decreases only by about 24.6%, which is much smaller than about 56.9% for the case of CO, while the decreasing for  $B_3$ CNTs keeps the same level as the case of CO (ca. 27%).

The preceding experimental results indicate that electron-deficient boron doping can also turn CNTs into metal-free ORR catalysts with positively shifted potentials and elevated reduction current, as well as high stability and immunity towards methanol crossover and CO poisoning.

To further understand the electrocatalytic activity of BCNTs, DFT calculations<sup>[22,23]</sup> were performed on boron-doped armchair (5,5) single-walled CNT (BCNT(5,5)) before and after  $O_2$  adsorption, including the geometry optimization and the subsequent natural bond orbital (NBO) analysis<sup>[24,25]</sup> (Supporting Information, S1.2). The results are shown in Figure 4 and the Supporting Information, S5. NBO charges were adopted in the population analysis.

In the optimized structures, the substitutional boron atom is three-coordinate ( $BC_3$ ), and exhibits  $sp_2$ -like hybridization in B–C  $\sigma$  bonds. The B–C  $\sigma$  bonds are considerably polarized owing to the larger electronegativity of carbon with respect to boron, which induces quite an amount (0.56e) of positive

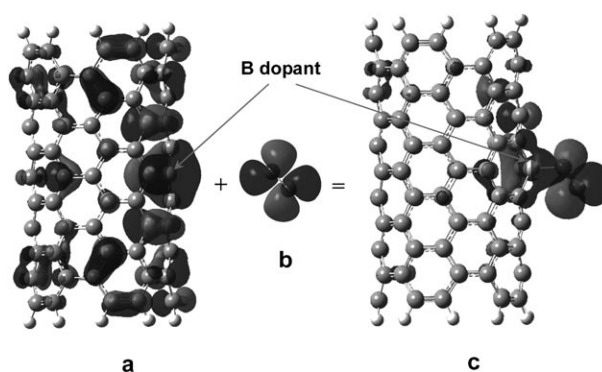


**Figure 4.** Important molecular orbitals involved in the  $O_2$  adsorption on BCNT(5,5). a) Spin-down HOMO–1 of BCNT(5,5). b) LUMO of triplet  $O_2$ . c) Spin-down HOMO–2 of  $O_2$ -BCNT(5,5).

charge on the boron atom (Supporting Information, S5, S6.1). This positively charged boron atom is favorable to capture of the  $O_2$  molecule, which is slightly negatively charged upon approaching the tube.<sup>[26]</sup> With a decreasing adsorption distance, the  $O_2$  molecule acquires more and more negative charge and the interaction between the boron and  $O_2$  is further strengthened, which eventually leads to a chemisorption of  $O_2$  on BCNT(5,5). In contrast to the N-doped CNTs (NCNTs), where  $O_2$  is adsorbed on the three carbon atoms neighboring the nitrogen dopant,<sup>[27]</sup> for the boron-doped CNTs,  $O_2$  is adsorbed on the boron dopant itself (Supporting Information, S6.2). Their common feature is that  $O_2$  adsorption favors the positively charged sites; that is, the carbon connected to the nitrogen dopant in NCNTs<sup>[7,27]</sup> and the boron dopant in BCNTs. For the pristine CNTs, this process could not be achieved as there is no charged site on the tube, and the ground state triplet  $O_2$  would have repulsion force with spin-singlet pristine CNTs owing to orbital mismatch (Supporting Information, S6.3). Thus, the positively charged boron dopant in BCNTs plays a significant role in enhancing the  $O_2$  chemisorption for the ORR.

Incorporating boron into carbon matrix could transform electron-deficient boron to electron-donating site by taking advantage of the rich  $\pi$  electrons in the carbon conjugated system. This is achieved through transferring the active electrons from C–C  $\pi^*$  antibonding orbital to vacant  $2p_z$  orbital of boron, as indicated in our NBO calculations. Consequently, a fraction of lone pair electrons with amount of 0.51 e appears in  $2p_z$  of the boron atom. The frontier orbital calculations suggest that this partially filled  $2p_z$  orbital constitutes the main protruding lobe in the two highest occupied molecular orbitals of BCNT(5,5); that is, HOMO and HOMO–1, acting as the electron-donating site for the ORR (Supporting Information, S6.4).

Upon adsorption, the lowest unoccupied molecular orbital (LUMO) of a triplet  $O_2$  (Figure 4b) would have maximal overlap with the protruding lobe of spin-down HOMO–1 of BCNT(5,5) (Figure 4a) to form an end-on adsorption (Figure 4c, Supporting Information, S7). This process is energetically favored, with an exothermic adsorption energy of –0.11 eV. With that, 0.45 e of charge transfers to  $O_2$ , accompanied by a elongation of the O–O bond length from 1.21 Å for the gas phase to 1.32 Å for the absorbed state, which indicates the weakening of the O–O bond of the absorbed  $O_2$ . The adsorption distance of 1.55 Å is much smaller than that of about 3.0 Å for the physisorption of  $O_2$  on CNT.<sup>[27,28]</sup> Thus, chemisorption occurs between  $O_2$  and BCNT(5,5), which is the precondition for the ORR. It is worth noting that upon adsorption, the charge on the boron atom does not change much (from 0.56 e to 0.61 e), while the adjacent carbon atoms lose quite an amount of electrons (0.46 e; Supporting Information, S5). This result indicates that the 0.45 e accumulated charge in  $O_2$  actually comes from the carbon atoms, with boron acting as a bridge.

Based on the preceding analysis, the origin of the catalytic ability of BCNTs for ORR could be rationally understood; that is, the positively charged boron dopant induces chemisorptions of  $O_2$  on BCNTs; some  $\pi^*$  electrons in the conjugated system accumulate on the boron dopant, which

can easily transfer to the chemisorbed  $O_2$  molecules for the ORR with boron as a bridge. When the boron dopant is in oxidized states, that is,  $BC_2O$  or  $BCO_2$ , this mechanism is still valid (Supporting information, S8). Thus boron doping plays the crucial role in forming this advanced metal-free ORR catalyst.

In conclusion, a new kind of metal-free electrocatalysts of boron-doped carbon nanotubes has been developed that exhibits quite a good performance for the ORR in electrocatalytic activity, stability, and immunity towards methanol crossover and CO poisoning. The electrocatalytic performances are improved progressively with increasing boron content, as reflected in the increased reduction current and the positively shifted onset and peak potentials (Figure 2). Theoretical calculations indicate that boron doping enhances the  $O_2$  chemisorption on BCNTs. The electrocatalytic ability of BCNTs for ORR stems from the electron accumulation in the vacant  $2p_z$  orbital of boron dopant from the  $\pi^*$  electrons of the conjugated system; thereafter, the transfer readily occurs to the chemisorbed  $O_2$  molecules with boron as a bridge. The transferred charge weakens the O–O bonds and facilitates the ORR on BCNTs. The experimental progress and theoretical understanding in this study point out the two key factors for the doped CNTs as metal-free ORR catalysts: 1) Breaking the electroneutrality of CNTs to create the charged sites favorable for  $O_2$  adsorption despite whether the dopants are electron-rich (as N) or electron-deficient (as B); and 2) effective utilization of carbon  $\pi$  electrons for  $O_2$  reduction. This work suggests further exploration of the metal-free electrocatalysts in the heteroatom-doped carbon nanostructures with one or more dopants, such as B, N and P, which should be a hopeful strategy for developing the advanced practical electrocatalysts for fuel cells.

Received: February 21, 2011

Revised: April 11, 2011

Published online: June 17, 2011

**Keywords:** boron · carbon nanotubes · electrocatalysts · fuel cells · oxygen reduction reaction

- [1] H. A. Gasteiger, N. M. Markovic, *Science* **2009**, *324*, 48–49.
- [2] M. Winter, R. J. Brodd, *Chem. Rev.* **2004**, *104*, 4245–4269.
- [3] A. Kowal, M. Li, M. Shao, K. Sasaki, M. B. Vukmirovic, J. Zhang, N. S. Marinkovic, P. Liu, A. I. Frenkel, R. R. Adzic, *Nat. Mater.* **2009**, *8*, 325–330.
- [4] V. R. Stamenkovic, B. S. Mun, M. Arenz, K. J. J. Mayrhofer, C. A. Lucas, G. F. Wang, P. N. Ross, N. M. Markovic, *Nat. Mater.* **2007**, *6*, 241–247.
- [5] J. Kim, Y. M. Lee, S. H. Sun, *J. Am. Chem. Soc.* **2010**, *132*, 4996–4997.
- [6] B. Winther-Jensen, O. Winther-Jensen, M. Forsyth, D. R. MacFarlane, *Science* **2008**, *321*, 671–674.
- [7] K. P. Gong, F. Du, Z. H. Xia, M. Durstock, L. M. Dai, *Science* **2009**, *323*, 760–764.
- [8] Y. F. Tang, B. L. Allen, D. R. Kauffman, A. Star, *J. Am. Chem. Soc.* **2009**, *131*, 13200–13201.
- [9] S. J. Jiang, Y. W. Ma, G. Q. Jian, H. S. Tao, X. Z. Wang, Y. N. Fan, Y. N. Lu, Z. Hu, Y. Chen, *Adv. Mater.* **2009**, *21*, 4953–4956.
- [10] S. H. Joo, S. J. Choi, I. Oh, J. Kwak, Z. Liu, O. Terasaki, R. Ryoo, *Nature* **2001**, *412*, 169–172.

- [11] C. Wang, M. Waje, X. Wang, J. M. Tang, R. C. Haddon, Y. S. Yan, *Nano Lett.* **2004**, *4*, 345–348.
- [12] Y. L. Hsin, K. C. Hwang, C. T. Yeh, *J. Am. Chem. Soc.* **2007**, *129*, 9999–10010.
- [13] Q. H. Yang, P. X. Hou, M. Unno, S. Yamauchi, R. Saito, T. Kyotani, *Nano Lett.* **2005**, *5*, 2465–2469.
- [14] W. K. Hsu, S. Firth, P. Redlich, M. Terrones, H. Terrones, Y. Q. Zhu, N. Grobert, A. Schilder, R. J. H. Clark, H. W. Kroto, D. R. M. Walton, *J. Mater. Chem.* **2000**, *10*, 1425–1429.
- [15] K. McGuire, N. Gothard, P. L. Gai, M. S. Dresselhaus, G. Sumanasekera, A. M. Rao, *Carbon* **2005**, *43*, 219–227.
- [16] Y. Hishiyama, H. Irumano, Y. Kaburagi, *Phys. Rev. B* **2001**, *63*, 245406.
- [17] L. S. Panchokarla, K. S. Subrahmanyam, S. K. Saha, A. Govindaraj, H. R. Krishnamurthy, U. V. Waghmare, C. N. R. Rao, *Adv. Mater.* **2009**, *21*, 4726–4730.
- [18] V. A. Paganin, E. Sitta, T. Iwasita, W. J. Vielstich, *J. Appl. Electrochem.* **2005**, *35*, 1239–1243.
- [19] F. Q. Liu, C. Y. Wang, *J. Electrochem. Soc.* **2007**, *154*, B514–B522.
- [20] R. F. Mann, J. C. Amphlett, B. A. Peppley, C. P. Thurgood, *J. Power Sources* **2006**, *161*, 768–774.
- [21] V. A. Sethuraman, S. Khan, J. S. Jur, A. T. Haug, J. W. Weidner, *Electrochim. Acta* **2009**, *54*, 6850–6860.
- [22] E. A. Carter, *Science* **2008**, *321*, 800–803.
- [23] Gaussian09. Revision A.02, M. J. Frisch, et al. (Gaussian, Inc., Wallingford CT, **2009**). See the Supporting Information, S11.
- [24] F. Weinhold, C. R. Landis, *Valency and Bonding: A Natural Bond Orbital Donor–Acceptor Perspective*, Cambridge University Press, New York, **2005**, pp. 55–60.
- [25] E. D. Glendening, A. E. Reed, J. E. Carpenter, F. Weinhold, NBO, Version 3.1 (Theoretical Chemistry Institute, Univ. Wisconsin, Madison WI, **2001**).
- [26] M. Grujicic, G. Cao, A. M. Rao, T. M. Tritt, S. Nayak, *Appl. Surf. Sci.* **2003**, *214*, 289–303.
- [27] X. Hu, Y. Wu, H. Li, Z. Zhang, *J. Phys. Chem. C* **2010**, *114*, 9603–9607.
- [28] P. Giannozzi, R. Car, G. Scoles, *J. Chem. Phys.* **2003**, *118*, 1003–1007.